PEROXIDE CROSS-LINKING OF EPDMs HAVING HIGH FRACTIONS OF ETHYLENIC UNITS

AMIN SHABANI,[1,2,*] XAVIER COLIN,[1] GREGORY MARQUE,[2] CAROLE MONCHY-LEROY[2]

[1]ARTS ET METIERS PARISTECH, LABORATOIRE PIMM, 151 BOULEVARD DE L'HÔPITAL, 75013 PARIS, FRANCE
[2]EDF R&D, LES RENARDIÈRES, AVENUE DES RENARDIÈRES, ECUELLES, 77818 MORET-SUR-LOING, FRANCE

RUBBER CHEMISTRY AND TECHNOLOGY, Vol. 87, No. 4, pp. 679–702 (2014)

ABSTRACT

The considerable amount of research in the literature has practically allowed the elucidation of the mechanism of peroxide cross-linking of ethylene–propylene–diene–monomer rubber (EPDM), which occurs through a radical chain reaction initiated by the thermal decomposition of the peroxide molecule. According to this radical chain reaction, all types of labile hydrocarbon bonds (i.e., allylic, methynic, and methylenic CH bonds) would be exposed to alkoxy radicals and involved in the formation of the elastomeric network. However, for high fractions of ethylenic units (typically $\geq$60 mol.%), simple chemical kinetics and thermochemical analyses have shown that the radical attack would essentially occur on the methylenic CH bonds. Starting from this assertion, a simplified mechanistic scheme has been proposed for the three commercial EPDMs under study. The corresponding kinetic model, derived from this new scheme by using the basic concepts of the chemical kinetics, provides access to the changes in concentration of the main reactive chemical functions (against exposure time), among which are double bonds and changes in cross-linking density. The validity of these predictions has been eventually successfully verified by five distinct analytical techniques frequently used for studying the cross-linking of rubbers. [doi:10.5254/rct.14.85989]

INTRODUCTION

Organic peroxides were used for the first time in 1915 as cross-linking agents of natural rubber.[1] Nowadays, a wide range of organic peroxides are used for cross-linking almost all types of linear hydrocarbon elastomers. The main advantage of using organic peroxides over sulfur compounds is the higher thermal stability of the resulting C–C bonds (their dissociation energy is of the order of 300–380 kJ·mol^{-1}) in comparison with the C–S (275 kJ·mol^{-1}) and S–S bonds (260 kJ·mol^{-1}), which leads to elastomeric networks with an improved resistance to thermal aging and, in particular, to thermal oxidation.[2]

That is the reason why organic peroxides are widely used for cross-linking ethylidene–propylene–diene monomers (EPDMs). These terpolymers contain an unsaturated monomer unit conjugationally isolated from the saturated backbone. The cross-linking mechanism of EPDMs by dicumyl peroxide (DCP) has been the subject of a high number of scientific works during the past half-century. Several experimental methods such as electron spin resonance (ESR), nuclear magnetic resonance, and differential scanning calorimetry (DSC) have been employed to tentatively elucidate this radical chain reaction.[3–8] There is a general consensus on the fact that this would be composed of the three main conventional steps (initiation, propagation, and termination):

- homolytic scission of the thermally unstable O–O bond (its dissociation energy is of the order of 120–150 kJ·mol^{-1})[9] of the peroxide molecule creating two alkoxy radicals,
- abstraction of labile hydrogens from the EPDM chain creating alkyl macroradicals, and
- bimolecular combination of macroradicals and their addition onto unsaturations, producing C–C cross-links.

*Corresponding author. Email: amin.shabani@outlook.com

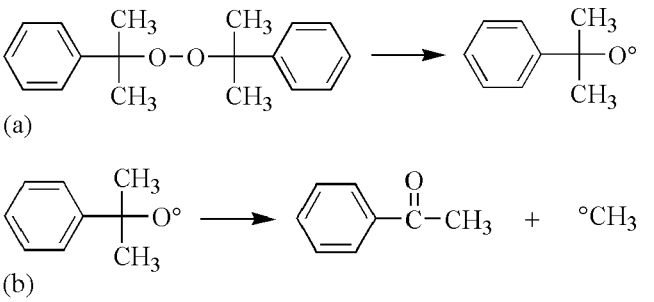

SCHEME 1. — (a) Homolytic scission of the O–O bond of DCP. (b) β-scission of cumyloxy radical.

As shown in Scheme 1a, the homolytic scission of the O–O bond of the DCP molecule creates two cumyloxy radicals.[10] These radicals can abstract a hydrogen atom on the polymer chain or can reorganize via a chain scission, better known as β-scission, to create a ketone (acetophenone) and a methyl radical (Scheme 1b). The latter can in turn abstract a hydrogen atom from the polymer chain to form an alkyl macroradical and a methane molecule (generally considered as the main volatile compound). The rate of the β-scission depends solely on temperature.[11]

According to the literature,[12] the radical attack would mainly occur on the methylenic CH bonds of the ethylenic units and the methynic CH bonds of the propylenic units of the EPDM chain, thus producing secondary and tertiary radicals, respectively (Scheme 2). Secondary radicals can easily couple in pairs to form tetrafunctional cross-links thanks to the lack of steric hindrance (Scheme 2a). As an indication, the cross-linking efficiency of a polyethylene has been estimated close to unity.[13] However, pairs of secondary radicals can also undergo a disproportionation, which decreases the cross-linking efficiency and creates unsaturations. On the other hand, the methyl groups attached to tertiary radicals (Scheme 2b) create a steric hindrance, thus lowering their probability of coupling. On the contrary, tertiary radicals can reorganize by β-scission, which provokes an apparent stronger decrease in the cross-linking efficiency.[14,15]

The side-chain third monomer can be involved in two competitive reactions: either the abstraction of allylic hydrogens or the addition of macroradicals onto unsaturations, with the latter contributing significantly to the cross-linking efficiency. Addition is favored when the double bond is terminal (i.e., located at the side-chain extremity), as in the case of vinyl

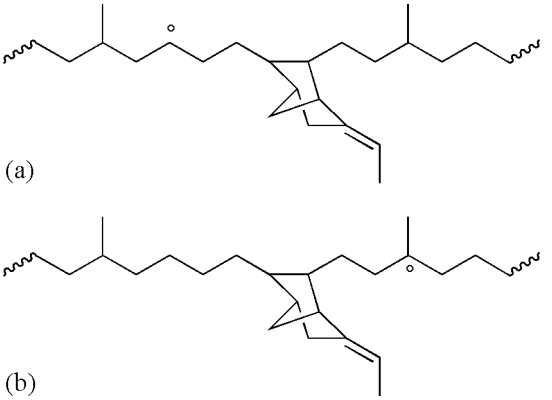

SCHEME 2. — (a) Secondary and (b) tertiary radicals in an EPDM chain.

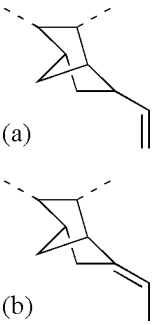

SCHEME 3. — (a) Vinyl norbornene. (b) Ethylidene norbornene.

norbornene (Scheme 3a). In contrast, abstraction of allylic hydrogens is favored when the double bond is internal, as in the case of ethylidene norbornene (ENB).[6,16] It is well known that, with this latter monomer, a nonnegligible part of unsaturations remains intact even after a complete peroxide cross-linking. As an example, a maximal conversion ratio of only 40 mol.% has been reported in the case of DCP.[17]

Thus, all types of labile hydrocarbon bonds (i.e., methylenic, methynic, and allylic CH bonds) would be involved in the formation of the EPDM network,[18] which would result in a complex mechanistic scheme. The number of possible main reactions, including hydrogen abstraction, bimolecular combination of macroradicals (both by coupling and disproportionation), and their addition onto unsaturations, and also possible side reactions, makes the mechanistic scheme very difficult to understand and elucidate. However, one can explore the different parts of this mechanism by carefully selecting different types of EPDM structures, for which the concentration of each type of labile hydrogen (and the corresponding macroradical) would be largely predominant over the other two.

With this intention, the present study will be focused on three commercial EPDMs having a high fraction of ethylenic units (typically $\geq$60 mol.%). On the basis of simple chemical kinetic and thermochemical analyses, it will be verified that the radical attack would essentially occur on methylenic CH bonds, thus providing the possibility of considerably simplifying the mechanistic scheme of peroxide cross-linking for the three EPDMs under study.

A kinetic model will be derived from this new mechanism and numerically solved by the commercial MATLAB software to access the changes in concentration (against exposure time) of the main reactive chemical functions and to deduce the changes in cross-linking density. The validity of these numerical simulations will be subsequently checked from several experimental techniques including spectrochemical (Fourier transform infrared spectroscopy [FTIR] in real-time) and rheometric (in molten/rubbery state) analyses, swelling of the elastomeric network (in an adequate solvent), and mechanical (uniaxial tensile) testing.

EXPERIMENTAL

SAMPLE PREPARATION AND CHARACTERIZATION

Three linear EPDMs containing ENB as diene monomer (denoted A, B, and C) were provided by Dow Chemical Co. According to industrial datasheets, they would have approximately the same chemical composition but different average macromolecular masses. More precise physicochemical characterizations were performed by conventional analytical techniques in our laboratory.

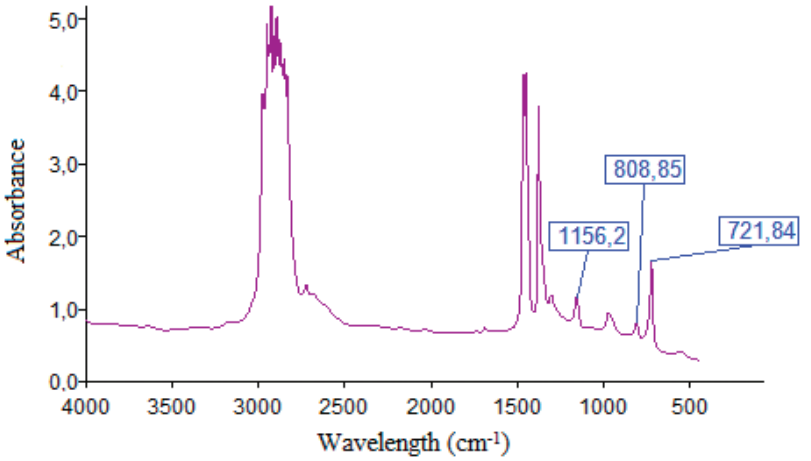

FIG. 1. — Typical FTIR spectrum of an un-cross-linked EPDM film.

Their chemical composition was determined on un-cross-linked 100 μm thick EPDM films by FTIR spectrophotometry in a transmission mode with a PerkinElmer Frontier spectrophotometer having a 4 cm^{-1} resolution. The three absorption bands of interest are indicated in the IR spectrum of Figure 1. Their main attributions and their corresponding molar extinction coefficients are given in Table I. Beforehand, a local deconvolution was performed to demonstrate that multiple absorptions at a given wave number can be reasonably neglected.

The concentrations of monomer units (i.e., ethylene, propylene, and ENB) were then calculated by using the classical Beer-Lambert's law. The results are given in Table II. These values will allow us to have precise data on the initial concentrations of the different chemical functions involved in the peroxide cross-linking of EPDMs.

The macromolecular structure was determined by high-temperature steric exclusion chromatography. The instrument was an Agilent PL GPC220 equipped by an Agilent PLgel Olexis guard column with a refractive index detector. The eluent was 1,2,4-trichlorobenzene with a common phenolic antioxidant. The nominal flow rate was 1.0 $mL \cdot min^{-1}$ at 160 °C, and the data were collected and analyzed using the Agilent cirrus software. In our case, the samples were prepared by adding 15 mL of eluent to 15 mg of EPDM and heating at 190 °C for 20 min. The solutions were cooled to 160 °C and then filtered through a 1.0 μm glass–fiber mesh. The numbers of average molar masses and polydispersity indices are given in Table III.

Linear EPDMs were mixed with different mass fractions (typically 1, 2.75, 3, 5.5, and 10 phr) of 99% pure DCP before cross-linking at 170 °C. As an indication, 3 phr corresponds to the peroxide content commonly used in industry for cross-linking EPDM insulators of electrical cables.

TABLE I
FUNCTIONAL ATTRIBUTION OF IR ABSORPTION BANDS AND CORRESPONDING MOLAR EXTINCTION COEFFICIENTS (ε)

Chemical group	ε,[a] $L \cdot mol^{-1} \cdot cm^{-1}$	Absorption, cm^{-1}
$-CH_3$ (propylene)	5[19]	1156
$-CH_2$- (ethylene)	2.6[19]	722
−C=C-H (ENB)	17.5[20]	809

[a] ε = molar extinction coefficient.

TABLE II
CONCENTRATIONS[a] OF MONOMER UNITS OF THE THREE LINEAR EPDMS UNDER STUDY

EPDM	Ethylene	Propylene	ENB
A	15.8	9.1	0.3
B	15.0	7.4	0.3
C	14.5	8.6	0.3

[a] Concentrations are expressed in $mol \cdot L^{-1}$.

ANALYTICAL TECHNIQUES

Several conventional analytical techniques were employed in this study to provide experimental data on the formation of EPDM networks at the molecular, macromolecular, and macroscopic scales throughout the peroxide cross-linking stage.

FTIR Spectrophotometry. — A specific device was inserted in the measure chamber of the FTIR spectrophotometer for monitoring in real-time the changes in chemical composition of the EPDM–DCP mixtures at 170 °C. This device consists of a pair of KBr windows lodged in a heating cell, while the temperature is controlled with a thermocouple. Films of the EPDM–DCP mixture of about 100 μm thick were positioned between the KBr windows and were rapidly heated to 170 °C. Once the temperature was equilibrated, FTIR spectra were recorded in a transmission mode every 30 s with a PerkinElmer Frontier spectrophotometer having a 4 cm^{-1} resolution. The test lasted 30 min in total in order to detect all possible chemical changes until the complete conversion of the cross-linking reaction.

DSC. — Differential calorimetry was used to measure the cross-linking enthalpy (ΔH_{total}) and the increase in glass transition temperature (T_g) of the EPDM–DCP mixtures after exposure at 170 °C. Samples of 5 to 10 mg were exposed under nitrogen at 170 °C for periods up to 30 min directly in the cavity of a TA Instruments Q1000 calorimeter. After this peroxide cross-linking stage, they were submitted to a temperature ramp from –80 °C to 235 °C at a heating rate of 10 $°C \cdot min^{-1}$ to be characterized. The ΔH_{total} of cross-linking and T_g, respectively, were taken as the area under the exothermic peak and the inflection point of the slope change in the DSC thermograms.

Rheometry. — Rheometry (in the molten/rubbery state) was used to monitor in real-time the changes in viscoelastic properties of EPDM–DCP mixtures at 170 °C. Dynamic time sweep tests were conducted under nitrogen with a coaxial parallel plate geometry having a plate diameter of 25 mm. The frequency was set at 100 $rad \cdot s^{-1}$ and the strain amplitude at 0.6%. Discs of EPDM–DCP mixture of 1.1 ± 0.1 mm thick were positioned between the plates of a Rheometrics Scientific ARES rheometer and were rapidly heated to 170 °C. They were maintained at this temperature for at least 30 min in order to reach the maximum cross-linking density of the EPDM networks. Attention

TABLE III
NUMBER OF AVERAGE MOLAR MASSES AND POLYDISPERSITY INDICES OF THE THREE LINEAR EPDMS UNDER STUDY

EPDM	M_n,[a] $g \cdot mol^{-1}$	Polydispersity
A	46,100	2.5
B	53,300	2.7
C	85,400	2.2

[a] M_n = number average molar mass.

was paid to the changes (against exposure time) in the loss G'' and storage G' shear moduli. As expected, for the formation of a three-dimensional structure, G'' decreases monotonously until almost vanishing, while G' increases until it reaches an asymptotic value. It was considered that this final value corresponds to the shear modulus of the fully cross-linked EPDM network.

Swelling. — Swelling (in an adequate solvent) was used to access directly the maximum cross-linking density of EPDM networks after complete peroxide cross-linking at 170 °C. Cubic samples of 30 to 50 mg (W_{ini}) were swelled in cyclohexane for 72 h at 25 °C. The cubes were then removed from the solvent, weighed in their swelled state (W_{sw}), and then placed under vacuum for 48 h at 40 °C to completely evaporate the solvent. Finally, the samples were weighed in their unswollen state (W_{gel}).

The swelling theory of Flory-Rehner[21–23] was used to evaluate the concentration of elastically active chains:

$$\nu = \frac{V_{r0} + \chi V_{r0}^2 + \ln(1 - V_{r0})}{V_s\left(\frac{2V_{r0}}{f} - V_{r0}^{1/3}\right)} \tag{1}$$

with

- ν: concentration of elastically active chains (mol·cm^{-3})
- V_{r0}: volume fraction of polymer in swelled gel
- V_s: molar volume of solvent (cm^3·mol^{-1})
- χ: Huggins' parameter of solvent–polymer interaction
- f: functionality of cross-link nodes

This approach is based on a homogeneous network: the result is an indicator of an average value of the cross-linking density. The volume fraction of swollen gel in the network V_{r0} is related to the solvent absorption factor k (ref 24):

$$V_{r0} = \frac{1}{1 + \frac{(k-1)\rho_p}{\rho_s}} \tag{2}$$

where ρ_p and ρ_s are the polymer (0.86 g·cm^{-3}) and solvent (0.78 g·cm^{-3}) densities at ambient temperature. k is given by

$$k = \frac{W_{sw}(\text{weight of swollen gel})}{W_{gel}(\text{weight of gel})} \tag{3}$$

and the gel fraction by

$$\%\text{gel} = \frac{W_{gel}(\text{weight of gel})}{W_{ini}(\text{initial weight})} \times 100 \tag{4}$$

The solvent–polymer interaction parameter is the sum of enthalpic and entropic components:

$$\chi = \chi_H + \chi_S \tag{5}$$

χ_H is the enthalpic interaction factor, which can be calculated by

$$\chi_H = (V_S/RT)(\delta_p - \delta_s)^2 \tag{6}$$

with δ_p and δ_s the solubility factors of polymer and solvent, respectively.

χ_s is a constant of about 0.35 ± 0.1 and, for a nonpolar solvent, is normally equal to 0.34.[25,26] So, the accepted equation will be

TABLE IV
SOLUBILITY PARAMETERS OF EPDM AND CYCLOHEXANE[27]

δ^a_{EPDM}, $(MPa)^{1/2}$	$\delta_{cyclohexane}$, $(MPa)^{1/2}$	$V^b_{cyclohexane}$, $cm^3 \cdot mol^{-1}$
16.3–18.0	16.7	108

[a] Solubility factor.
[b] Molar volume of solvent.

$$\chi \approx 0.34 + (V_S/RT)(\delta_p - \delta_s)^2 \tag{7}$$

The solubility parameters for EPDM and cyclohexane are given in Table IV.

To completely swell an elastomeric network with a solvent, their corresponding solubility parameters should be quasi-similar.[28] The discrepancy between the values of δ_p and δ_s tends to decrease the solvent absorption by the polymer.

Uniaxial Tensile Testing. — Uniaxial tensile testing was also used to access the maximum cross-linking density of EPDM networks after complete cross-linking at 170 °C. Dumbbell-shaped samples were cut with a cutting die from 2 mm thick plates. Their dimensions were 40 mm long, 4 mm wide, and 2 mm thick. The length of the grip section was 10 mm, and the gage length was 20 mm. The samples were positioned in the pneumatic grips of an Instron 4301 machine equipped with a static load cell supporting up to 100 kN. Tests have been carried out with a deformation rate of 1.25 s^{-1} in standard room conditions (i.e., 20 °C and relative humidity of 50%).

RESULTS AND DISCUSSION

PROPOSAL OF MECHANISTIC SCHEME

As explained in the Introduction section, the three linear EPDMs selected for this study present a largely higher fraction in ethylenic (63.9 ± 2.2 mol.%) than in propylenic (34.6 ± 2.1 mol.%) and ENB (1.28 ± 0.13 mol.%) units. A kinetic analysis was thus performed to determine the probability of the alkoxy radical attack on each type of labile hydrocarbon bonds and thus to see if the involvement of some of these bonds could be neglected in the general mechanistic scheme of peroxide cross-linking.

Such a radical attack can be schematized by the following reaction:

$$RO^\circ + P_iH \rightarrow ROH + P_i^\circ \qquad (k_i)$$

where RO° designates an alkoxy radical, P_iH the hydrocarbon bond under consideration, P_i° the resulting alkyl macroradical, and k_i the corresponding rate constant (expressed in $L \cdot mol^{-1} \cdot s^{-1}$).

The rate of this reaction is given by

$$r_i = k_i[RO^\circ][P_iH] \tag{8}$$

Let us consider the three labile hydrogen bonds of the EPDM chain and their corresponding alkyl radicals. Index "i" can be noted "s" for methylenic CH bonds and their corresponding secondary radicals, "t" for methynic CH bonds and their corresponding tertiary radicals, and "a" for allylic CH bonds and radicals. In this case, the probability p_s of the radical attack on methylenic CH bonds writes

$$p_s = \frac{r_s}{r_s + r_t + r_a} \tag{9}$$

that is,

TABLE V
ACTIVATION ENERGY (E_i), PREEXPONENTIAL FACTOR (K_{i0}), AND VALUE AT 170 °C OF THE PROPAGATION RATE CONSTANT OF THERMAL OXIDATION IN LINEAR HYDROCARBON POLYMERS

Rate constant	E_i,[a] $kJ \cdot mol^{-1}$	k_{i0},[b] $L \cdot mol^{-1} \cdot s^{-1}$	k_i, at 170 °C $L \cdot mol^{-1} \cdot s^{-1}$
k_s [29–31]	73	150×10^8	37
k_t [32]	66	3×10^8	6
k_a [33]	63	56×10^8	210

[a] Activation energy.
[b] Preexponential factor.

$$p_s = \frac{k_s[P_sH]}{k_s[P_sH] + k_t[P_tH] + k_a[P_aH]} \tag{10}$$

Expressions of p_t and p_a can be obtained by circular permutation of indexes.

Values of $[P_iH]$ were directly determined from Table II. In contrast, it was found that the too few values of k_i available in the literature are highly dependent on the mathematical form of the kinetic model used for their determination. That is the reason why the values of k_i chosen for the determination of p_i were taken from our own set of data on the propagation of thermal oxidation ($P\text{-}OO^\circ + P_iH \rightarrow POOH + P_i^\circ$) in linear hydrocarbon polymers. These values are reported in Table V. This approach is justified by the fact that Expression 10 is independent of the type and concentration of the involved radicals.

The resulting values of p_i are reported in Table VI.

These results suggest that the radical attack would mainly occur on methylenic CH bonds because more than 90% of the formed macroradicals would be of secondary type. Starting from this assertion, the following simplified mechanistic scheme, based on a single reactive site (the methylenic CH bonds noted PH), has been proposed for the DCP cross-linking of the three linear EPDMs under study:

(I) Initiation: $DCP \rightarrow 2\ ArMe_2C\text{–}O^\circ$ (ΔH_1, k_1)
(II) β-scission: $ArMe_2C\text{–}O^\circ \rightarrow ArMeC{=}O + H_3C^\circ$ (ΔH_2, k_2)
(III) Propagation: $ArMe_2C\text{–}O^\circ + PH \rightarrow ArMe_2C\text{–}OH + P^\circ$ (ΔH_3, k_3)
(IV) Propagation: $H_3C^\circ + PH \rightarrow CH_4 + P^\circ$ (ΔH_4, k_4)
(V) Addition: $P^\circ + F_{ENB} \rightarrow P\text{–}P + P^\circ$ (ΔH_5, k_5)
(VI) Termination: $P^\circ + {}^\circP \rightarrow \gamma_6 P\text{–}P + (1-\gamma_6)PH + (1-\gamma_6)F$ (ΔH_6, k_6)

where DCP designates the DCP; $ArMe_2C\text{–}O^\circ$ a cumyloxy radical; ArMeC=O the acetophenone; $ArMe_2C\text{–}OH$ the cumyl alcohol; PH a methylene CH bond; P° an alkyl radical; F_{ENB} the ethylidene

TABLE VI
PROBABILITY[a] OF THE RADICAL ATTACK ON THE LABILE HYDROCARBON BONDS OF THE THREE LINEAR EPDMS UNDER STUDY

EPDM	Methylenic	Methynic	Allylic
A	91.2	4.0	4.8
B	91.1	3.5	5.4
C	90.3	4.1	5.6

[a] Expressed in mol.%.

TABLE VII
BOND DISSOCIATION ENERGIES[33,36,37]

Chemical bond	ΔH, kJ·mol^{-1}	Chemical bond	ΔH, kJ·mol^{-1}
O–O	148	H_3C–H	415
C–CH_3	351	–CH=CH–	(2×) 303
C–O	341	>CH–C	315
>CH–H	393	>CH–CH<	328
O–H	460	⩾C–C⩽	301

double bond; F a vinylene double bond; P–P a tetrafunctional cross-link node, which, for sake of simplicity, will be hereafter denoted by X; and ΔH_i and k_i the enthalpies and rate constants of the elementary reactions under consideration.

It can be noticed that termination (VI) is a balance reaction taking into account both the coupling and disproportionation of pairs of alkyl radicals. γ_6 and $(1-\gamma_6)$ are the respective yields of cross-linking and disproportionation. According to our own results on the kinetic modeling of the thermal and radiochemical aging of polyethylene and its ethylene propylene rubber copolymers, both yields would be relatively close since $\gamma_6 \approx 0.5$.[34,35]

Three distinct approaches were used to check the validity of such a mechanistic scheme based on a strong but partly justified (given the high fraction in ethylenic units) assumption:

- The thermochemical approach allows calculating the enthalpies (ΔH_i) of the elementary reactions from bond dissociation energies. The overall cross-linking enthalpy is the algebraic sum of these elementary enthalpies. Its value can be checked by DSC.
- The kinetic approach allows deriving, from the previous mechanistic scheme, a kinetic model giving access to the concentration changes (against exposure time) of the main reactive chemical functions. These simulations can be checked by FTIR spectrometry in real time.
- The physical approach allows deducing, from these changes in chemical composition, the changes in cross-linking density. These last predictions can be checked by several analytical techniques (differential calorimetry, rheometry, mechanical spectrometry, swelling, uniaxial tensile testing, etc.).

The next sections are dedicated to the development and application of these approaches.

CHECKING THE MECHANISTIC SCHEME VALIDITY

Thermochemical Approach. — A rapid review of available data from organic chemistry allowed compiling the dissociation energies of the different chemical bonds involved in the previous mechanistic scheme (Table VII).

The balance enthalpy ΔH_i of each elementary reaction ($i = 1...6$) was calculated by the following method. As a first example, the β-scission of one cumyloxy radical (II) leads to the breaking of one C–CH_3 bond and the formation of one C–O bond, so that

$$\Delta H_2 = \Delta H_{C-CH3} - \Delta H_{C-O} = 351 - 341 = 10\,\mathrm{kJ \cdot mol^{-1}} \qquad (11)$$

As a second example, each propagation event (III) leads to the breaking of one >CH–H bond and the formation of one O–H bond, so that

TABLE VIII
ELEMENTARY ENTHALPIES OF THE SIMPLIFIED MECHANISTIC SCHEME OF EPDM CROSS-LINKING BY DCP

Elementary reaction	(I)	(II)	(III)	(IV)	(V)	(VI)
ΔH_i, kJ·mol^{-1}	148	10	−67	−22	−12	−316

$$\Delta H_3 = \Delta H_{>CH-H} - \Delta H_{O-H} = 393 - 460 = -67\,kJ \cdot mol^{-1} \quad (12)$$

As a third and last example, each termination event (VI) leads to the formation of a γ_6 >CH–CH< bond (by coupling) and $(1-\gamma_6)$ –CH=CH– bond (by disproportionation), so that

$$\Delta H_6 = \gamma_6 \Delta H_{>CH-CH<} - (1-\gamma_6)\Delta H_{CH=CH} = -328\gamma_6 - 303(1-\gamma_6) \quad (13)$$

Taking $\gamma_6 = 0.5$, the following comes finally: $\Delta H_6 = -316$ kJ·mol^{-1}.

Values of ΔH_i determined by this method are reported in Table VIII.

The overall cross-linking enthalpy (expressed in kJ per mole of DCP) is the algebraic sum of these elementary enthalpies:

$$\Delta H_{total} = \Delta H_1 + 2\alpha\Delta H_2 + 2(1-\alpha)\Delta H_3 + 2\alpha\Delta H_4 + \Delta H_5 + \Delta H_6 \quad (14)$$

with α the partition coefficient between reaction paths (II) and (III):

$$\alpha = \frac{[ArMeC=O]}{[ArMeC=O] + [ArMe2C-OH]} \quad (15)$$

The value of the coefficient α is difficult to determine by FTIR analysis because the absorption band of alcohols in the 3300–3600 cm^{-1} region is rather broad and poorly defined, and also it may interfere with the absorption band of usual molecules also bearing hydroxyl groups (in particular, sorbed water). In addition, the absorption band of unsaturated ketones at 1690 cm^{-1} reaches its saturation limits at the early periods of cross-linking. That is the reason why, in a first approach, the value of α was estimated from spectrochemical data on the thermal decomposition of DCP in cumene at moderate temperature.[38] The extrapolation of these data to 170 °C by a linear regression gave $\alpha/(1-\alpha) = 2.22$, which led finally to $\alpha = 0.69$ (Figure 2).

It was reported in the literature[39] and confirmed by our own experimental results (see the next section) that a nonnegligible part of ethylidene double bonds remains intact even after complete peroxide cross-linking. To take into account this peculiarity of ENB units, a conversion ratio x_{ENB}, corresponding to the number of moles of double bonds consumed per initial moles of DCP (x_{ENB}), has been introduced into Eq. 14:

$$\Delta H_{total} = \Delta H_1 + 2\alpha\Delta H_2 + 2(1-\alpha)\Delta H_3 + 2\alpha\Delta H_4 + x_{ENB}\Delta H_5 + \Delta H_6 \quad (16)$$

By replacing ΔH_i by their respective values (see Table VIII) and taking $\alpha = 0.69$, it becomes finally

$$\Delta H_{total} = -226 - 12x_{ENB} \quad (17)$$

The cross-linking enthalpy has been measured by DSC for a series of EPDM-DCP mixtures at 170 °C to determine the average value of the conversion ratio x_{ENB} for the three EDPM networks under study. Results are reported in Tables IX and X, respectively.

It can be noticed that ΔH_{total} and x_{ENB} are of the same order of magnitude for the three EPDM networks under study, which suggests that they have almost the same cross-linking density. This coherence was naturally expected because of the very close chemical structure of the three starting linear EPDMs.

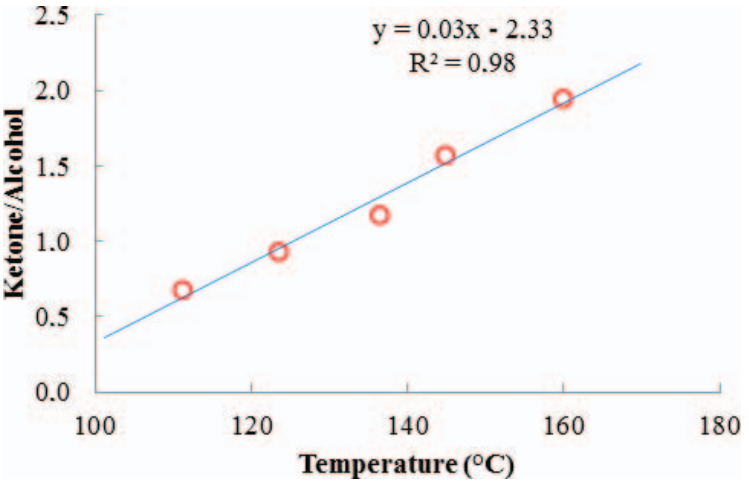

FIG. 2. — Ratio $\alpha/(1-\alpha)$ during the thermal decomposition of DCP between 110 and 160 °C in cumene.[38]

Kinetic Approach. — The following system of differential equations was derived from the simplified mechanistic scheme of EPDM cross-linking by DCP:

$$\frac{d[DCP]}{dt} = -k_1[DCP] \tag{18}$$

$$\frac{d[ArMe_2CO^\circ]}{dt} = 2k_1[DCP] - k_2[ArMe_2CO^\circ] - k_3[ArMe_2CO^\circ][PH] \tag{19}$$

$$\frac{d[H_3C^\circ]}{dt} = k_2[ArMe_2CO^\circ] - k_4[H_3C^\circ][PH] \tag{20}$$

$$\frac{d[P^\circ]}{dt} = k_3[ArMe_2CO^\circ][PH] + k_4[H_3C^\circ][PH] - 2k_6[P^\circ]^2 \tag{21}$$

$$\frac{d[F_{ENB}]}{dt} = -k_5[P^\circ][F_{ENB}] \tag{22}$$

TABLE IX
CROSS-LINKING ENTHALPY[a] FOR EPDMS MIXED WITH DIFFERENT CONCENTRATIONS OF DCP

DCP, phr	A	B	C
10	238	241	236
5.5	247	241	244
2.75	238	249	262
1	254	237	227
Average	246 ± 8	243 ± 6	240 ± 15

[a] Expressed in $kJ \cdot mol^{-1}$ of DCP.

TABLE X
CONVERSION RATIO x_{ENB} AT 170 °C OF THE THREE EPDM NETWORKS UNDER STUDY

EPDM	x_{ENB}, mol/mol
A	1.7 ± 0.6
B	1.5 ± 0.5
C	1.3 ± 0.5

$$\frac{d[ArMeC{=}O]}{dt} = k_2[ArMe_2CO^\circ] \tag{23}$$

$$\frac{d[CH_4]}{dt} = k_4[H_3C^\circ][PH] \tag{24}$$

$$\frac{d[ArMe_2COH]}{dt} = k_3[ArMe_2CO^\circ][PH] \tag{25}$$

$$\frac{d[X]}{dt} = k_5[P^\circ][F_{ENB}] + \gamma_6 k_6[P^\circ]^2 \tag{26}$$

Initial conditions (at $t = 0$) are

$$[DCP] = [DCP]_0 \tag{27}$$

$$[ArMe_2CO^\circ] = [H_3C^\circ] = [P^\circ] = 0 \tag{28}$$

$$[F_{ENB}] = [F_{ENB}]_0 \tag{29}$$

$$[PH] = [PH]_0 \tag{30}$$

$$[ArMeC{=}O] = [CH_4] = [ArMe_2C{-}OH] = 0 \tag{31}$$

$$[X] = 0. \tag{32}$$

This system of nine nonlinear differential equations was implemented in the commercial MATLAB software and numerically solved using a semi-implicit algorithm (ODE23s solver) especially dedicated to stiff problems of chemical kinetics. The values of the different rate constants (k_i) were collected in the literature and are provided in Table XI.

As an example, the changes in the chemical composition of an EPDM A-DCP mixture (with a DCP content of 3 phr commonly used in the electrical cable industry) during its cross-linking at 170 °C are reported in Figures 3 to 6. These simulations have been compared with experimental data obtained by FTIR spectrometry in real time. It can be observed that there is a satisfying agreement between theory and experiment without the need for an additional assumption or adjustable parameter, which allows proving the validity of both the proposed mechanistic scheme and the corresponding kinetic model at the molecular scale.

These results call for the following comments:

The initiation step (I) (i.e., the homolytic scission of the O–O bond of the DCP molecule), was the subject of several studies.[9,40–42] According to these publications, the

TABLE XI
KINETIC PARAMETERS FOR MODELING EPDM CROSS-LINKING BY DCP

Reaction	k_{i0},[a] s^{-1} or $mol \cdot L^{-1} \cdot s^{-1}$	E_i,[b] $kJ \cdot mol^{-1}$	k_i,[c] s^{-1} or $mol \cdot L^{-1} \cdot s^{-1}$
(I)[40]	2.7×10^{12}	122	1.1×10^{-2}
(II)[44]	1.7×10^{13}	64	4.9×10^{6}
(III)[47]	7.5×10^{10}	53	4.2×10^{4}
(IV)[49]	1.6×10^{15}	58	2.3×10^{8}
(V)[48]	2.3×10^{6}	14	5.1×10^{4}
(VI)[50]	1.8×10^{11}	0	1.8×10^{11}

[a] k_{i0} = preexponential factor.
[b] E_i = activation energy.
[c] k_i = rate constant at 170 °C.

initiation rate constant would obey an Arrhenius law with a preexponential factor (k_{10}) in the range of 10^{12}–10^{14} s^{-1} and activation energy (E_1) of the order of 120–146 $kJ \cdot mol^{-1}$. The best fit of DCP depletion (Figure 3) was obtained with $k_{10} = 2.7 \times 10^{12}$ and $E_1 = 122$ $kJ \cdot mol^{-1}$, that is, with Arrhenius parameters very close to the values reported in ref 40. It results in a rate constant $k_1 = 1.1 \times 10^{-2}$ s^{-1} at 170 °C.

The rearrangement by β-scission of cumyloxy radicals (II) was the subject of refs 43 and 44. The best fit for the acetophenone formation (Figure 4) was obtained with Arrhenius parameters $k_{20} = 1.7 \times 10^{13}$ and $E_2 = 64$ $kJ \cdot mol^{-1}$, that is, leading to a rate constant $k_{02} = 4.9 \times 10^{6}$ s^{-1} at 170 °C, in accordance with ref 44. It can be seen that the kinetic model convincingly fits the first experimental data in the early periods of cross-linking. For longer periods of peroxide cross-linking, the predictive value of the model cannot be checked because, unfortunately, the IR absorption band of acetophenone at 1690 cm^{-1} has reached its saturation limit, making impossible the determination of concentration values. Nevertheless, it describes the rapid slowdown in the acetophenone formation: the acetophenone concentration reaches an asymptotic value when the DCP concentration vanishes in the reaction medium. At the present time, the model does not predict the physical loss of acetophenone by evaporation, because it was assumed that this phenomenon is very slow due to the rather large size of the molecule (120 $g \cdot mol^{-1}$). However, it should not be forgotten that the evaporation rate is an increasing function of temperature and concentration. Billingham's law[45,46]

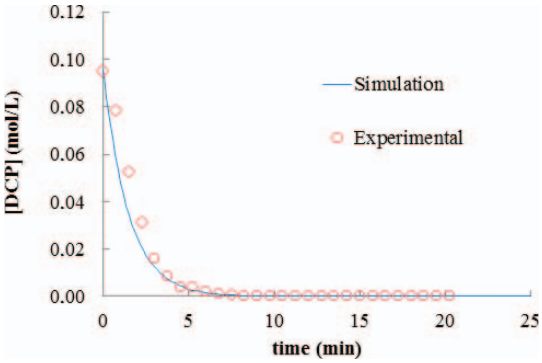

FIG. 3. — Changes in the peroxide concentration during the cross-linking at 170 °C of a linear EPDM A mixed with 3 phr of DCP.

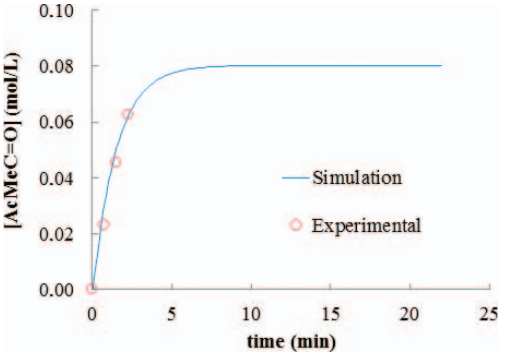

FIG. 4. — Changes in the acetophenone concentration during the cross-linking at 170 °C of a linear EPDM A mixed with 3 phr of DCP.

could be used as a boundary condition (in Eq. 31) to predict a slight decrease in the concentration of acetophenone at very long term if necessary.

Cumyloxy radicals can, as well, abstract a labile hydrogen atom along the EPDM chain to form a cumyl alcohol and a macroradical (III). A value of $k_3 = 4.2 \times 10^4$ L·mol^{-1}·s^{-1} was found at 170 °C by using Arrhenius parameters $k_{30} = 7.5 \times 10^{10}$ L·mol^{-1}·s^{-1} and $E_3 = 53$ kJ·mol^{-1} in accordance with ref 47. In this case, the maximal cumyl alcohol concentration is about 1.1×10^{-1} mol·L^{-1} (Figure 5; i.e., a fairly low value), which explains the difficulties in detecting the characteristic IR absorption band of hydroxyl groups (given the poor sensibility thershold of the FTIR spectrophotometry).

Based on the maximal values of acetophenone and cumyl alcohol concentrations determined by numerical simulation, a value of 0.72 has been calculated for the partition coefficient α between elementary reactions (II) and (III) (see Eq. 15). This value is very close to that previously extrapolated (0.69) from literature data.[30]

Macroradicals add onto ethylidene double bonds to form tetrafunctional cross-link nodes (V). Because the molecular structures of ethylidene and isoprene double bonds are not so dissimilar (>C=CH–), it was assumed that the Arrhenius parameters k_{50} and E_5 should be of the same order of magnitude as the values determined for linear polyisoprene in a previous study.[48] The simulations of ENB depletion obtained by using Arrhenius parameters $k_{50} = 2.3 \times 10^6$ and $E_5 = 11$ kJ·mol^{-1}

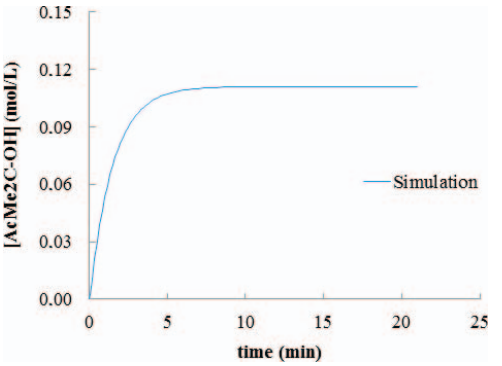

FIG. 5. — Changes in the cumyl alcohol concentration during the cross-linking at 170 °C of a linear EPDM A mixed with 3 phr of DCP.

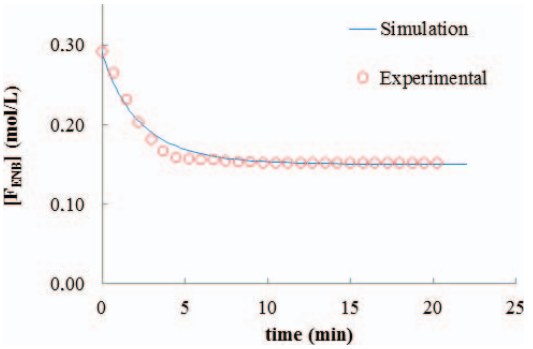

FIG. 6. — Changes in the ethylidene double bond concentration during the cross-linking at 170 °C of a linear EPDM A mixed with 3 phr of DCP.

(i.e., a rate constant $k_5 = 5.1 \times 10^4$ mol·L^{-1}·s^{-1} at 170 °C) are reported in Figure 6. It can be seen that the kinetic model satisfyingly fits the experimental results.

As a conclusive remark, it has been seen that the kinetic model successfully describes the concentration changes (against exposure time) of the main reactive chemical functions during the peroxide cross-linking of EPDM-DCP mixtures. However, based on Eq. 26, the kinetic model can be subsequently used to predict the final cross-linking density (X) of the EPDM networks. This point is the subject of the next sections.

PHYSICAL APPROACH

An EPDM network can be characterized by only two structural quantities well known to have a direct impact on mechanical properties[51–53]:

- The concentration ν of the subchains connected by both of their extremities to cross-link nodes, namely, the "elastically active chains." It is related to the cross-link functionality f and concentration X by

$$\nu = \frac{f}{2} X \tag{33}$$

- The concentration b of the subchains connected by only one extremity to cross-link nodes, namely, the "dangling chains." It is equal to the concentration of chain ends of the starting linear polymer:

$$b = \frac{2\rho}{M_n} \tag{34}$$

where ρ is the polymer density.

Since the starting linear EPDMs have an average molar mass higher than 15 kg·mol^{-1} (see Table III), the corresponding EPDM networks have a very low value of b ($= [3.1 \pm 0.9] \times 10^{-2}$ mol·L^{-1}). This value is about one order of magnitude lower than that usually reported for ν ($= [3.6 \pm 0.6] \times 10^{-1}$ mol·L^{-1}) in the literature for such an elastomeric network.[7,54,55] As a consequence, the fully cross-linked EPDM networks could be considered as "ideal networks" (i.e., with almost no flaws such as dangling chains or even closed loops).

Four distinct analytical techniques were used to determine the ν values of the three fully cross-linked EPDM networks under study. These results were subsequently compared with numerical simulations.

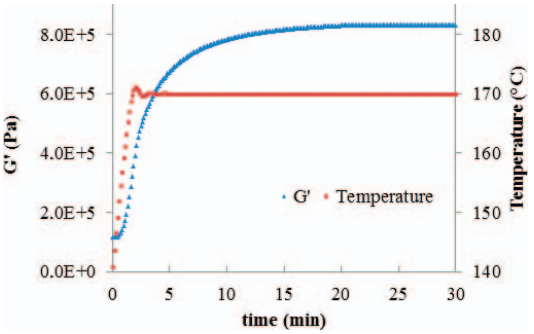

FIG. 7. — Changes in the storage modulus during the cross-linking at 170 °C of a linear EPDM A mixed with 3 phr of DCP.

Rheometry. — The theory of rubber elasticity establishes a relationship between the storage modulus G' of an elastomeric network and its concentration ν of elastically active chains[21]:

$$G' = \nu \rho R T \tag{35}$$

where R is the perfect gas constant and T the absolute temperature.

The polymer density ρ depends on temperature. In a first approximation, its variation with temperature can be approximated by[56]

$$\rho_T = \frac{\rho_{298K}}{1 + 3\alpha_l(T - 298)} \tag{36}$$

where α_l is the linear thermal expansion coefficient.

Taking $\rho = 0.86\ \text{g·cm}^{-3}$ at 298 K and $\alpha_l = 2.3 \times 10^{-4}\ \text{K}^{-1}$,[57] we get $\rho = 0.78\ \text{g·cm}^{-3}$ at 170 °C for the three EPDM networks under study.

In the case of an ideal network, ν is equal to the reciprocal molar mass of elastically active chains M_C:

$$\nu = \frac{1}{M_C} \tag{37}$$

Figure 7 shows the changes in G' of the EPDM A-DCP mixture (with a DCP content of 3 phr) during its cross-linking at 170 °C in the rheometer cavity. As expected for the formation of a three-dimensional structure, G' increases until it reaches an asymptotic value $G'_\infty \approx 1.1$ MPa after about 20 min of cross-linking time. From a practical point of view, it was considered that the EPDM network is fully cross-linked when G' is worth 98% of its maximal value (i.e., after only 15 min). The corresponding value of G' was then used to determine the values of ν and M_C from Eqs. 35 and 37, respectively.

The values of G'_∞, ν, and M_C thus determined for the three EPDM networks under study are reported in Table XII.

Differential Calorimetry. — The Di Marzio theory can be used to establish a relationship between the glass transition temperature T_g of an elastomeric network and its cross-link concentration X (ref 58):

$$T_g = \frac{T_{g1}}{1 - K_{DM} F X} \tag{38}$$

where T_{g1} is the T_g of the initial linear EPDM, K_{DM} the universal constant, and F the chain dynamic stiffness (or flex parameter). For a tetrafunctional network with an aliphatic backbone, K_{DM} is of the

TABLE XII
SHEAR MODULUS AND CONCENTRATION AND MOLAR MASS OF ELASTICALLY ACTIVE CHAINS DETERMINED BY EQS. 35–37 FOR THE THREE FULLY CROSS-LINKED EPDM NETWORKS UNDER STUDY

EPDM	G'_{∞},[a] MPa	ν,[b] mol·L^{-1}	M_C,[c] g·mol^{-1}
A	1.13	4.4×10^{-1}	2.64×10^{3}
B	0.95	3.7×10^{-1}	3.14×10^{3}
C	0.99	3.8×10^{-1}	3.06×10^{3}

[a] Storage modulus.
[b] Concentration of elastically active chains.
[c] Mass of elastically active chains.

order of 6.[59] The flex parameter is defined as the molar mass of a given entity (chain or a subchain) divided by the number of flexible bonds contained in this entity. The latter has been calculated using the data from Table II. It was found that F is of the order of 17 for the three EDPM networks under study (Table XIII).

Figure 8 shows the changes in T_g of the three EPDM-DCP mixtures (with a DCP content of 3 phr) during their cross-linking at 170 °C in the calorimeter cavity. As expected for the formation of a three-dimensional structure, T_g increases until it reaches an asymptotic value $T_{g\infty} = -48.5 \pm 0.5$ °C after about 20 min of cross-linking time. At this stage, it is important to notice the large experimental scattering on $T_{g\infty}$ that did not allow an accurate determination of the values of X and ν, from Eqs. 38 and 33, respectively, but only their orders of magnitude.

The average values of $T_{g\infty}$, X, and ν thus determined for the three EPDM networks under study are reported in Tables XIII and XIV. It can be seen that the orders of magnitude of ν are relatively close to those found previously by rheometry (except for EPDM A). However, these results should be considered with caution given their too large uncertainties. That is the reason why, in the following sections, more accurate analytical methods have been employed for the determination of ν.

Swelling. — Table XV gives the values of the solvent uptake factor and gel fraction of the three fully cross-linked EPDM networks under study in cyclohexane at room temperature. It can be noticed that these values are very close.

Based on these data and the value of the Huggins' parameter determined for the EPDM cyclohexane mixture at 25 °C, the corresponding concentrations of elastically active chains were calculated according to Eq. 1. The average values of ν are reported in Table XVI within an interval related to $\chi = 0.38 \pm 0.03$.

TABLE XIII
UNIVERSAL CONSTANT (K_{DM}), FLEX PARAMETER (F), AND CONCENTRATIONS OF CROSS-LINK NODES (X) AND ELASTICALLY ACTIVE CHAINS (ν) DETERMINED BY EQ. 38 FOR THE THREE FULLY CROSS-LINKED EPDM NETWORKS UNDER STUDY

EPDM	A	B	C
K_{DM}	6	6	6
F, g·mol^{-1}	17.3	17.1	17.4
X, mol·L^{-1}	$(1.4 \pm 2.0) \times 10^{-1}$	$(1.9 \pm 1.0) \times 10^{-1}$	$(1.9 \pm 1.0) \times 10^{-1}$
ν, mol·L^{-1}	$(2.9 \pm 4.0) \times 10^{-1}$	$(3.9 \pm 2.0) \times 10^{-1}$	$(3.9 \pm 3.0) \times 10^{-1}$

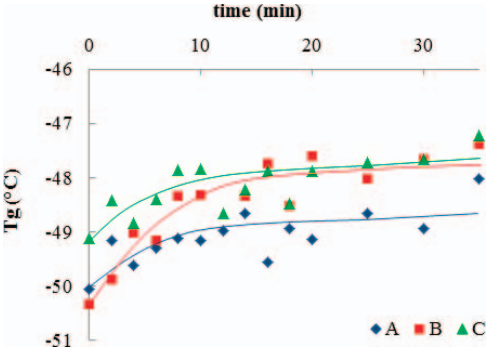

FIG. 8. — Changes in the glass transition temperature during the cross-linking at 170 °C of the three linear EPDMs under study mixed with 3 phr of DCP.

Uniaxial Tensile Testing. — The tensile stress–strain curves obtained for the three fully cross-linked EPDM networks under study were analyzed in two different ways. In a first (coarse grain) approach, the slope of the tensile curves at the origin (i.e., when the strain tends toward zero) was determined graphically to deduce the value of the Young's modulus E. According to the classical theory of rubber elasticity, E is related to the concentration of elastically active chains ν by

$$E = \lim_{\varepsilon \to 0} \frac{\sigma}{\varepsilon} = 3\nu\rho R\,T \tag{39}$$

This equation implies that the Young's modulus is three times the shear modulus at low strain ($E = 3G$), which effectively justified the case for an incompressible material. The corresponding values of ν for the three EPDMs under study are reported in Table XVII.

In a second (more precise) approach, the entire tensile stress-elongation curves were tentatively reproduced by the Mooney–Rivlin equation[60,61]:

$$\sigma = 2\left(\lambda - \frac{1}{\lambda^2}\right)\left(C_1 + \frac{C_2}{\lambda}\right) \tag{40}$$

where λ is the elongation and C_1 and C_2 are empirical parameters for which some authors tried to give a physical meaning.[62,63]

The rearrangement of this equation gives the following[64]:

$$\frac{\sigma}{2(\lambda - \lambda^{-2})} = \left(C_1 + \frac{C_2}{\lambda}\right) = f\left(\frac{1}{\lambda}\right) \tag{41}$$

Thus, the plotting of the ratio $\frac{\sigma}{2(\lambda-\lambda^{-2})}$ versus the reciprocal elongation $\frac{1}{\lambda}$ should be a straight line for which the slope and the intercept with the y-axis should give direct access to the values of C_2 and C_1,

TABLE XIV
AVERAGE VALUES OF THE GLASS TRANSITION TEMPERATURE BEFORE AND AFTER COMPLETE CROSS-LINKING AT 170 °C OF THE THREE LINEAR EPDMS UNDER STUDY MIXED WITH 3 PHR OF DCP

EPDM	A	B	C
T_{gl}, °C	−52	−52	−52
$T_{g\infty}$, °C	−48.7 ± 0.5	−47.7 ± 0.4	−47.7 ± 0.4

TABLE XV
SOLVENT UPTAKE FACTOR (K) AND GEL FRACTION OF THE THREE FULLY CROSS-LINKED EPDM NETWORKS UNDER STUDY IN CYCLOHEXANE AT 25 °C

EPDM	k	% gel
A	3.04	98
B	3.08	98
C	3.05	98

respectively. Then, the introduction of these values into Eq. 35 should allow the perfect reproduction of the tensile stress-elongation curve.

This methodology was applied for the three fully cross-linked EPDM networks under study. As an example, the straight line and tensile stress-elongation curve obtained for the EPDM B network are displayed in Figures 9a and 9b, respectively. The values of C_2 and C_1 thus determined are reported in Table XVIII.

To calculate the corresponding value of the Young's modulus, the deformation ($\varepsilon = 1 - \lambda$) was introduced into Eq. 35:

$$\sigma = 2 \left(1 + \varepsilon - \frac{1}{(1+\varepsilon)^2}\right)\left(C_1 + \frac{C_2}{1+\varepsilon}\right) \tag{42}$$

At low strain ($\varepsilon << 1$), this equation can be rewritten:

$$\sigma = 6\varepsilon(C_1 + C_2) \tag{43}$$

so that

$$E = \lim_{\varepsilon \to 0} \frac{\sigma}{\varepsilon} = 6(C_1 + C_2) \tag{44}$$

The values of E thus determined are also reported in Table XVIII. It can be concluded that both approaches gave comparable results.

PREDICTION OF THE CHANGES IN CROSS-LINKING DENSITY

On the basis of the results obtained by four different analytical methods (rheometry, differential calorimetry, swelling, and uniaxial tensile testing), the physicochemical approach has confirmed the initial conclusions of the thermodynamic approach: the three EPDM networks under study have almost the same maximal cross-linking density. They can be

TABLE XVI
CONCENTRATION OF ELASTICALLY ACTIVE CHAINS (ν) DETERMINED BY EQS. 1–4 FOR THE THREE FULLY CROSS-LINKED EPDM NETWORKS UNDER STUDY

EPDM	ν, mol·L^{-1}
A	$(4.4 \pm 0.6) \times 10^{-1}$
B	$(4.2 \pm 0.6) \times 10^{-1}$
C	$(4.3 \pm 0.5) \times 10^{-1}$

TABLE XVII
CONCENTRATION OF THE ELASTICALLY ACTIVE CHAINS (ν) DETERMINED GRAPHICALLY (SEE TEXT) FROM THE TENSILE STRESS–STRAIN CURVES FOR THE THREE FULLY CROSS-LINKED EPDM NETWORKS UNDER STUDY

EPDM	E,[a] MPa	ν, mol·L^{-1}
A	2.3 ± 0.1	$(3.7 \pm 0.2) \times 10^{-1}$
B	2.5 ± 0.1	$(4.0 \pm 0.2) \times 10^{-1}$
C	2.4 ± 0.1	$(3.8 \pm 0.2) \times 10^{-1}$

[a] Young's modulus.

assimilated to a single ideal network having concentrations of elastically active chains $\nu = (4.0 \pm 1.0) \times 10^{-1}$ mol·L^{-1} and cross-link nodes $X = (2.0 \pm 0.5) \times 10^{-1}$ mol·L^{-1} (since cross-link nodes are tetrafunctional [$f = 4$]).

At this stage of investigation, it seems interesting to test the predictive value of the kinetic model at the macromolecular scale. For this purpose, Eq. 26 has been used to calculate the changes in the cross-link concentration of the EPDM A-DCP mixture (with a DCP content of 3 phr) at 170 °C. In Figure 10, it can be seen that X increases until it reaches an asymptotic value of 1.9×10^{-1} mol·L^{-1}. This maximal value is fairly close to the above experimental cross-link concentration. This is a first sound argument in favor of the validity of the kinetic model.

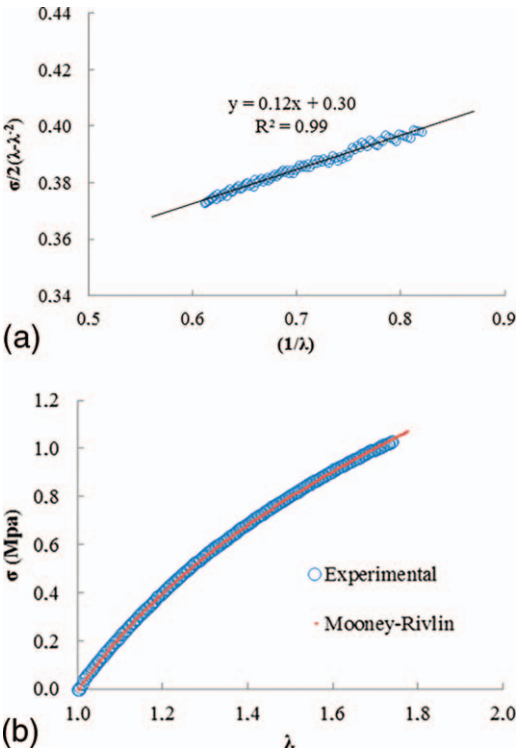

FIG. 9. — Tensile behavior of the fully cross-linked EPDM B network: (a) plot of $\frac{\sigma}{2(\lambda - \lambda^{-2})}$ versus $\frac{1}{\lambda}$. (b) Comparison of the Mooney–Rivlin equation with experimental data.

TABLE XVIII
CONCENTRATION OF THE ELASTICALLY ACTIVE CHAINS DETERMINED NUMERICALLY (SEE TEXT) FROM THE ENTIRE TENSILE STRESS-ELONGATION CURVES FOR THE THREE FULLY CROSS-LINKED EPDM NETWORKS UNDER STUDY

EPDM	E, MPa	v, mol·L^{-1}	C_1[a]	C_2[b]
A	2.2 ± 0.2	$(3.4 \pm 0.4) \times 10^{-1}$	0.29	0.07
B	2.5 ± 0.2	$(4.0 \pm 0.4) \times 10^{-1}$	0.30	0.12
C	2.5 ± 0.2	$(3.9 \pm 0.4) \times 10^{-1}$	0.33	0.08

[a,b] Empirical parameters of the Mooney–Rivlin equation.

However, an important question remains open: is this kinetic model still valid for EPDM rubbers containing significantly different concentrations of diene monomers and, in particular, for ethylene–propylene–monomer rubbers (EPMs)? To answer this last question, Eq. 26 has been used to tentatively predict the final cross-link concentration of EPDM-DCP and EPM-DCP mixtures (with DCP contents of 1.25, 2.5, 5, and 10 phr) at 170 °C reported by Orza.[17] Both linear polymers have been selected for this numerical calculation because they have a fraction of ethylenic units (59.0 and 64.4 mol.%, respectively) of the same order of magnitude as our three commercial EPDMs. As an indication, their respective concentrations of monomer units are recalled in Table XIX.

The results of all simulations have been plotted in Figure 11. It can be seen that the kinetic model predicts accurately the experimental cross-link concentration of both types of fully cross-linked EP(D)M networks over the whole range of initial mass fraction of DCP under study. It can be thus now concluded that the validity of the kinetic model is fully demonstrated.

CONCLUSIONS

The complex mechanistic scheme currently accepted for the peroxide cross-linking of EPDMs has been simplified in the case of EPDMs having a high fraction of ethylenic units (typically $\geq$60 mol.%) after having checked, from simple chemical kinetic and thermochemical analyses, that more than 90% of the radical attack would occur on the methylenic CH bonds.

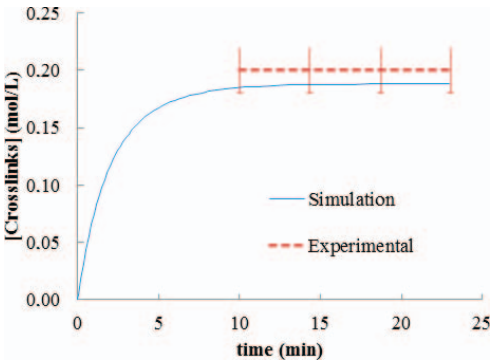

FIG. 10. — Changes in the cross-link concentration during the cross-linking at 170 °C of a linear EPDM A mixed with 3 phr of DCP.

TABLE XIX
CONCENTRATION[a] OF MONOMER UNITS OF THE TWO LINEAR EP(D)MS STUDIED BY ORZA[17]

EP(D)M	Ethylene	Propylene	ENB
O1	17.7	9.6	0.15
O2	16.1	11.2	0

[a] Concentrations are expressed in mol·L^{-1}.

A kinetic model has been derived from this new scheme and solved numerically by using the values of the elementary rate constants found in the literature. Its validity has been successfully checked at both molecular and macromolecular scales for three commercial EPDMs. On one hand, it was shown that the kinetic model convincingly fits the concentration changes of the main reactive chemical functions monitored by FTIR spectrophotometry in real time. On the other hand, it was shown that it predicts accurately the cross-linking density of the fully cross-linked EPDM networks measured by four different analytical techniques: rheometry (in molten/rubbery state), differential calorimetry, swelling (in cyclohexane), and uniaxial tensile testing. Finally, the validity of the kinetic model has been checked for two other types of EP(D)Ms found in the literature.

The challenge is now to perform the same kind of study on additional types of EP(D)Ms (e.g., those having high fractions in propylenic units) to verify the validity of a different but complementary part of the complex mechanistic scheme of peroxide cross-linking and also to begin to generalize the kinetic model to all EP(D)M structures.

ACKNOWLEDGEMENTS

This work has been performed in the framework of the Nuclear Polymer Project (NPP), whose aim is the lifetime prediction of EPDM insulators of electrical cables used in a nuclear plant environment. The authors are grateful to the Material Aging Institute (MAI) and EDF R&D for their financial support.

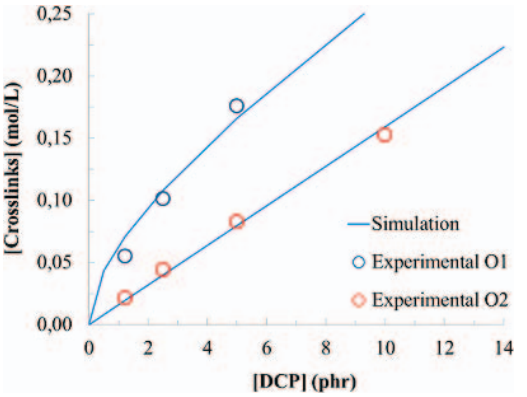

FIG. 11. — Cross-link concentration versus initial mass fraction of DCP for the two types of fully cross-linked EP(D)M networks studied by Orza.[17]

REFERENCES

[1]I. I. Ostromislensky and J. Russ, *Phys. Chem*. **47**, 1472 (1915).

[2]X. Colin, G. Teyssedre, and M. Fois, "Ageing and Degradation of Multiphase Polymer Systems," in *Handbook of Multiphase Polymer Systems*, A. Boudenne, L. Ibos, Y. Candau, and S. Thomas, Eds.; John Wiley & Sons, Ltd., Chichester, U.K., 2011.

[3]L. J. Loan, *Polym Sci. A Polym. Chem*. **2**, 3053 (1964).

[4]D. Brazier and N. Schwartz, *Thermochim. Acta* **39**, 7 (1980).

[5]R. C. Keller, RUBBER CHEM. TECHNOL. **61**, 238 (1987).

[6]M. Zachary, S. Camara, A. C. Whitwood, B. C. Gilbert, M. van Duin, R. J. Meier, and V. Chechik, *Eur. Polym. J*. **44**, 2099 (2008).

[7]R. A. Orza, P. C. M. M. Magusin, V. M. Litvinov, M. van Duin, and M. A. J. Michels, *Macromolecules* **40**, 8999 (2007).

[8]R. Orza, P. C. M. M. Magusin, V. M. Litvinov, M. van Duin, and M. A. J. Michels, *Macromolecules* **42**, 8914 (2009).

[9]D. Robbins, A. J. Almquist, D. C. Timm, J. I. Brand, and R. E. Gilbert, *Macromolecules* **28**, 8729 (1995).

[10]M. Van Duin and H. G. Dikland, RUBBER CHEM. TECHNOL. **76**, 132 (2003).

[11]D. Brazier and G. Nickel, RUBBER CHEM. TECHNOL. **48**, 661 (1975).

[12]L. D. Loan, *J. Polym. Sci. A Polym. Chem*. **2**, 3053 (1964).

[13]A. Rijke and L. Mandelkern, *Macromolecules* **4**, 594 (1971).

[14]E. Borsig, M. Lazár, A. Fiedlerová, L. Hrčková, M. Rätzsch, and A. Marcinčin, *Macromol. Symp*. **176**, 289 (2001).

[15]B. Dickens, *J. Polym. Sci. A Polym. Chem*. **20**, 1169 (1982).

[16]M. Vallat, F. Ruch, and M. David, *Eur. Polym. J*. **40**, 1575 (2004).

[17]R. A. Orza, P. C. M. M. Magusin, V. M. Litvinov, M. van Duin, and M. A. J. Michels, *Macromol. Symp*. **230**, 144 (2005).

[18]R. Orza, "Investigation of Peroxide Crosslinking of EPDM Rubber by Solid-State NMR 2008," Ph.D. Thesis, Technische Universiteit Eindhoven, 2008.

[19]H. L. McMurry and V. Thornton, *Anal. Chem*. **24**, 318 (1952).

[20]A. Rivaton, S. Cambon, and J. L. Gardette, *Nucl. Instrum. Methods Phys. Res. Sect. B* **227**, 343 (2005).

[21]P. J. Flory, "Molecular Weight Distribution in Nonlinear Polymers and the Theory of Gelation," in *Principles of Polymer Chemistry*, Cornell University Press, Ithaca, NY, 1953.

[22]P. J. Flory, *Trans. Faraday Soc*. **57**, 829 (1961).

[23]P. J. Flory, *Macromolecules* **12**, 119 (1979).

[24]M. Celina and G. A. George, *Polym. Degrad. Stab*. **48**, 297 (1995).

[25]R. F. Blanks and J. M. Prausnitz, *Ind. Eng. Chem. Fund*. **3**, 1 (1964).

[26]R. L. Scott and M. J. Magat, *Polym. Sci. A Polym. Chem*. **4**, 555 (1949).

[27]J. Brandrup, E. H. Immergut, and E. A. Grulke, *Polymer Handbook*, John Wiley & Sons, Ltd., Chichester, U.K., 1999.

[28]B. A. Miller-Chou and J. L. Koenig, *Prog. Polym. Sci*. **28**, 1223 (2003).

[29]N. Khelidj, X. Colin, L. Audouin, J. Verdu, C. Monchy-Leroy, and V. Prunier, *Polym. Degrad. Stab*. **91**, 1593 (2006).

[30]N. Khelidj, X. Colin, L. Audouin, J. Verdu, C. Monchy-Leroy, and V. Prunier, *Polym. Degrad. Stab*. **91**, 1598 (2006).

[31]X. Colin, B. Fayolle, L. Audouin, and J. Verdu, *Polym. Degrad. Stab*. **80**, 67 (2003).

[32]S. Sarrabi, X. Colin, and A. Tcharkhtchi, *Materiaux & Techniques*, **96**, 281 (2008).

[33]J. G. Calvert and J. N. Pitts, *Photochemistry*, Vol. 1, John Wiley & Sons, New York, 1966.

[34]N. Khelidj, X. Colin, L. Audouin, J. Verdu, C. Monchy-Leroy, and V. Prunier, *Polym. Degrad. Stab*. **91**, 1593 (2006).

[35]X. Colin, E. Richaud, J. Verdu, C. Monchy-Leroy, *Radiat. Phys. Chem*. **79**, 365 (2010).

[36]R. T. Morrison and R. N. Boyd, *Organic Chemistry*, 6th ed., Prentice-Hall, Upper Saddle River, NJ, 1992.

[37]P. Kelter, M. Mosher, and A. Scott, *Chemistry: The Practical Science,* Vol. 10, Brooks/Cole, Boston, 2007.

[38]H. C. Bailey and G. W. Godin, *Trans. Faraday Soc*. **52**, 68 (1956).

[39]R. A. Orza, P. C. M. M. Magusin, V. M. Litvinov, M. van Duin, and M. A. J. Michels, *Macromolecules* **42**, 8914 (2009).

[40]K. Dixon, "Decomposition Rates of Organic Free Radical Initiators," in *Polymer Handbook*, 4th ed., J. Brandrup, E. H. Immergut, and E. A. Grulke, Eds., John Wiley & Sons, Ltd, Chichester, UK, 1999.

[41]V. L. Antonovskii and S. L. Khursan, *Russ. Chem. Rev*. **72**, 939 (2007).

[42]K. Wu, H. Hou, and C. J. Shu, *Therm. Anal. Calorim*. **83**, 41 (2006).

[43]M. Buback, M. Kling, and S. Z. Schmatz, *Phys. Chem*. **219**, 1205 (2005).

[44]A. Baignee, et al., *J. Am. Chem. Soc*. **105**, 6120 (1983).

[45]N. C. Billingham and P. D. Calvert, "The Physical Chemistry of Oxidation and Stabilization of Polyolefins," in *Development in Polymer Stabilization*, Vol. 3, G. Scott, Ed., Applied Science Publishers, London, 1980.

[46]N. C. Billingham and P. D. Calvert, *J. Appl. Polym. Sci*. **24**, 357 (1979).

[47]E. T. Denisov and I. B. Afanas'ev, *Oxidation and Antioxidants in Organic Chemistry and Biology*, CRC Press, Boca Raton, FL, 2005.

[48]X. Colin, L. Audouin, and J. Verdu, *Polym. Degrad. Stab*. **92**, 886 (2007).

[49]B. Likozar and M. Krajnc, *Polym. Eng. Sci*. **49**, 60 (2009).

[50]N. Khelidj, X. Colin, L. Audouin, C. Monchy-Leroy, and V. P. Prunier, *Polym. Deg. Stab*. **91**, 1593 (2006).

[51]X. Colin, L. Audouin, and J. Verdu, *Polym. Degrad. Stab*. **92**, 906 (2007).

[52]T. Colclough, J. Cunneen, and G. Higgins, *J. Appl. Polym. Sci*. **12**, 295 (1968).

[53]L. J. Mullins, *Polym. Sci. A Polym. Chem*. **19**, 225 (1956).

[54]E. Planes, L. Chazeau, G. Vigier, and J. Fournier, *Polymer* **50**, 4028 (2009).

[55]J. M. Kranenburg, M. Van Duin, and U. S. Schubert, RUBBER CHEM. TECHNOL. **84**, 101 (2011).

[56]D. W. Van Krevelen and K. Te Nijenhuis, *Properties of Polymers: Their Correlation with Chemical Structure; Their Numerical Estimation and Prediction from Additive Group Contributions*, 4th ed., Elsevier Science, Amsterdam, 2009.

[57]J. E. Mark, *Polymer Data Handbook*, Vol. 2., 2nd ed., Oxford University Press, New York, 2009.

[58]V. Bellenger, J. Verdu, and E. Morel, *J. Polym. Sci. B Polym. Phys*. **25**, 1219 (1987).

[59]W. D. Cook, *Eur. Polym. J*., **14**, 715 (1978).

[60]M. Mooney, *J. Appl. Phys*. **11**, 582 (1940).

[61]R. Rivlin, *Phil. Trans. R. Soc. A* **241**, 379 (1948).

[62]M. Llorente and J. Mark, *Macromolecules* **13**, 681 (1980).

[63]J. E. Mark, *Physical Properties of Polymers Handbook*, Springer, New York, 2007.

[64]F. Horkay and G. B. McKenna, *Physical Properties of Polymers Handbook*, Springer, New York, 2007.